



# Simulation of Diesel Fuel Injection System (Effects of Basic Characteristic Values on Injection Performances)

メタデータ	言語: eng 出版者: 公開日: 2010-04-06 キーワード (Ja): キーワード (En): 作成者: Hattori, Hiroshi, Hirako, Yoshio メールアドレス: 所属:
URL	<a href="https://doi.org/10.24729/00008717">https://doi.org/10.24729/00008717</a>

# Simulation of Diesel Fuel Injection System

## (Effects of Basic Characteristic Values on Injection Performances)

Hiroshi HATTORI\* and Yoshio HIRAKO\*\*

(Received June 14, 1975)

### Abstract

In diesel engines, performance and thermal efficiency are greatly dependent on fuel injection characteristics. Therefore, a theoretical estimation of injection characteristics under various operating conditions including abnormal injection would contribute to develop or to design a new fuel injection system.

As a first step for this analytical estimation, this paper describes the details of a method of theoretical analysis and effects of various fundamental factors on injection characteristics. An example comparing the calculated results with the experimental results is also shown.

### 1. Introduction

Recent trend of diesel engines is still towards higher speed and higher power. Performance factors such as torque, speed control, fuel consumption and exhaust smoke are largely dependent on injection characteristics. It would, therefore, be very favourable in developing and designing a new fuel injection system, if the effects of various parameters on injection processes such as a change of pressures in the system and the rate of fuel injection could be correctly predicted. Many attempts<sup>1-8)</sup> have so far been made to predict these processes graphically or numerically, and with a development of electronic computers, fairly accurate simulations of the system have become possible. In most of these studies, however, the pressure in the pipe line and the rate of injection are compared with the experimental results. Few papers<sup>9-11)</sup> have dealt with abnormal injection such as secondary injection and cyclic irregularity of injection, because it is generally said that secondary injection may cause after-burning or incomplete combustion and therefore the loss of engine performance and that irregular injection may involve harmful influences on the operation of engines and the durability of injection systems.

Accordingly, the authors are interested in how abnormal injection occurs and how it can be avoided. The purpose of this investigation is to analyze the injection processes theoretically and to find out the reasons to cause abnormal injection and the possibilities to avoid it. As a first step for this investigation, this paper describes a method of theoretical analysis and the calculated results for various fundamental factors on which the injection characteristics are greatly dependent. In this simu-

---

\* Research Student, Department of Mechanical Engineering, College of Engineering.

\*\* Department of Mechanical Engineering, College of Engineering.

lation, the fuel injection system is analyzed according to the method given in Reference (6).

## 2. Analytical Procedure of Fuel Injection System

### 2.1 Assumptions.

Before theoretical modeling of the injection system, the following assumptions are made:

- (1) Temperature and sound velocity in a fuel are constant and physical properties of the fuel such as density, viscosity and surface tension do not change during one injection cycle.
- (2) Evaporation of the fuel in boids is not considered.
- (3) Fuel concentrated in an element has no inertia, but is only elastic, and it is considered to be always in a perfect isobaric condition.
- (4) Sealing between mechanical components is considered perfect and deformation of these components is also ignored.

### 2.2 Definitions of fundamental functions.

The pressure, the rate of flow and the motions of plunger and valves can be represented by differential equations with respect to time or cam angle. For the simplicity of description, the pressure and the rate of flow are defined as follows: *Pressure*: When the fuel of a volume ( $V+s$ ) is compressed into a container of a volume ( $V$ ), the pressure in it can be represented by  $E \cdot s/V$ . That is,

$$p = \begin{cases} E \cdot s/V & (s \geq 0) \\ 0 & (s < 0) \end{cases} \quad (1)$$

Hereafter, this equation can be expressed symbolically by

$$p = pres(s, V) \quad (1)'$$

In this equation, if the quantity of the compressed fuel ( $s$ ) is negative, the pressure is zero, viz. boids generate in the container. In addition, by using the quantity of compressed fuel as a fundamental variable in place of the pressure, Eq. (1) or Eq. (1)' can express not only the presence of boids, but also the quantity of them.

*Rate of flow*: When there is a pressure difference  $\Delta p$  between both sides of an orifice with an effective area ( $\mu F$ ), the rate of flow ( $q$ ) through this orifice is

$$q = \mu F \sqrt{2\Delta p / \rho}$$

and in order to hold the above equation even for negative  $\Delta p$ , it is better to write

$$q = \mu F \Delta p / \sqrt{\rho |\Delta p| / 2} \quad (2)$$

This equation is also expressed symbolically,

$$q = flow(\mu F, \Delta p) \quad (2)'$$

As  $\Delta p$  approaches zero in the above equation,  $\partial q/\partial p$  approaches infinity, namely diverges. In order to avoid this divergence, the term  $\sqrt{\rho|\Delta p|/2}$  is transformed to  $\sqrt{\rho|\Delta p|/2+\varepsilon}$  where  $\varepsilon$  is a quite small positive quantity.

### 2.3 Pumping chamber.

The quantity of compressed fuel in the pumping chamber ( $s_k$ ) is represented as a function of plunger stroke ( $H_k$ ), lift of delivery valve ( $H_v$ ) and rates of flow into and out of the pumping chamber ( $q_{ek}$  and  $q_{kv}$ , respectively). The differential equation with respect to time ( $t$ ) is

$$\frac{ds_k}{dt} = F_k \frac{dH_k}{dt} + q_{ek} - F_v \frac{dH_v}{dt} - q_{kv} \quad (3)$$

where

$$q_{ek} = \text{flow}(\mu_e F_e, p_e - p_k) \quad (4)$$

$$q_{kv} = \text{flow}(\mu_v F_v, p_k - p_v) \quad (5)$$

$$p_k = \text{pres}(s_k, V_{ko} - F_k H_k + F_v H_v) \quad (6)$$

### 2.4 Delivery valve chamber.

The quantity of compressed fuel in the delivery valve chamber ( $s_v$ ) is determined by the motion of valve and the rates of flow into and out of this chamber. In a similar manner to the pumping chamber, the following equation can be obtained.

$$\frac{ds_v}{dt} = F_v \frac{dH_v}{dt} + q_{kv} - q_1 \quad (7)$$

where  $q_1$  is the rate of flow out of the delivery valve chamber to the first element of the injection pipe line. The differential equation of the valve motion is

$$m_v \frac{d^2 H_v}{dt^2} = F_v(p_k - p_v) - c_v(H_v - H_{vo}) - K_v \frac{dH_v}{dt} \quad (8)$$

and then

$$p_v = \text{pres}(s_v, V_{vo} - F_v H_v + F_l L/2N) \quad (9)$$

where  $F_l L/2N$  will be discussed in the next section.

### 2.5 Injection pipe line.

When the cross sectional area of the pipe line is constant and there are no booids in it, the equation of continuity and that of motion are

$$\frac{\partial p}{\partial t} + E \frac{\partial w}{\partial x} = 0, \quad \rho \frac{\partial w}{\partial t} + \frac{\partial p}{\partial x} + D = 0$$

where  $w$  is the velocity of flow,  $D$  is the pressure drop per unit length,  $t$  is the time,  $x$  is the distance and  $E$  is the elastic modulus of fuel. These equations can be solved under given initial and boundary conditions by the characteristic curve method considering pressure waves. However, since the rate of pressure rise of the fuel in

the pipe line is not so large and high frequency components of pressure waves are very small, we can practically assume that the pipe line is divided into a finite number of elements and each of them is regarded as a lumped parameter system.

By dividing the length of the equivalent pipe line (the length from the outlet of the delivery chamber to the inlet of nozzle chamber) into  $N$  as in Fig. 1, we can obtain the equation of motion in the pipe line.

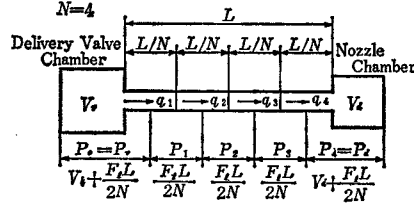


Fig. 1. An example of division of pipe line

$$\frac{dq_i}{dt} = \frac{F_i N}{L} (p_{i-1} - p_i) - 2\zeta q_i \quad (i=1, 2, \dots, N) \quad (10)$$

where  $\zeta$  is the resistance coefficient which is assumed to be equal to that of the laminar flow,

$$\zeta = 16\eta/\rho d^2 \quad (11)$$

where  $\eta$  is the coefficient of viscosity.

With the quantity of the compressed fuel  $s_i$  in the  $i$ -th element, the following equation can be derived:

$$p_i = \text{pres}(s_i, F_i L/N) \quad (12)$$

The pressures  $p_0$  and  $p_N$  at the both ends of the pipe line are equal to  $p_v$  and  $p_d$ , respectively, and the volume  $F_i L/2N$  is added to the volume in Eqs. (9) and (17). Then,  $s_i$  is represented as follows:

$$\frac{ds_i}{dt} = q_i - q_{i+1} \quad (i=1, 2, \dots, N-1) \quad (13)$$

## 2.6 Injection nozzle.

According to the same consideration as at the delivery valve, the quantity of compressed fuel ( $s_d$ ) at the nozzle chamber is

$$\frac{ds_d}{dt} = q_N - q - F_N \frac{dH_d}{dt} \quad (14)$$

In this equation  $q$  corresponds to the rate of injection at the nozzle tips,

$$q = \text{flow}(\mu_d F_d, p_d - p_z) \quad (15)$$

where  $p_z$  is the back pressure at the nozzle, namely the pressure in the engine cylinder.

The equation of motion for the nozzle needle valve can be represented by

$$\frac{d^2 H_d}{dt^2} = \frac{F_N - F_s}{m_d} p_d + \frac{F_p}{m_d} p_z - \frac{c_d}{m_d} (H_d + H_{d0}) - \frac{K_d}{m_d} \frac{dH_d}{dt} \quad (16)$$

where the pressure in the nozzle chamber is

$$p_d = \text{pres}(s_d, V_{d0} + F_N H_d + F_L L / 2N) \quad (17)$$

The cumulative injection quantity ( $Q$ ) per one injection cycle at the nozzle tips can be obtained from the rate of injection  $q$  in Eq. (14):

$$\frac{dQ}{dt} = q \quad (18)$$

### 3. Calculation Method and Programming

It can be easily found that some basic equations described in the previous section can be expressed by simultaneous ordinary differential equations of variables:  $s_k$ ,  $s_v$ ,  $H_v$ ,  $dH_v/dt$ ,  $q_1, \dots, q_N$ ,  $s_1, s_2, \dots, s_{N-1}$ ,  $s_d$ ,  $H_d$ ,  $dH_d/dt$  and  $Q$ . When these variables are replaced with  $y_i$  ( $i=1, 2, \dots, m$ ), the following equations can be obtained:

$$\frac{dy_i}{dt} = f_i(t, y_1, y_2, \dots, y_m) \quad (i=1, 2, \dots, m)$$

Then, function  $f_i$  can be calculated when  $y_1, y_2, \dots, y_m$  and  $t$  are given. If the pipe line is divided into eight elements, we have to consider the following 23 variables, that is,  $s_i$  ( $i=1, 2, \dots, 7$ ),  $q_i$  ( $i=1, 2, \dots, 8$ ),  $s_k$ ,  $s_v$ ,  $H_v$ ,  $dH_v/dt$ ,  $s_d$ ,  $H_d$ ,  $dH_d/dt$  and  $Q$ . In this case, the simultaneous ordinary differential equations have 23 dimensions. The solutions of these equations can be obtained by numerical integration when initial conditions are given. In this paper, we use the method of Runge-Kutta-Gill for numerical integration.

However, as the residual pressure or the quantity of boids in the injection

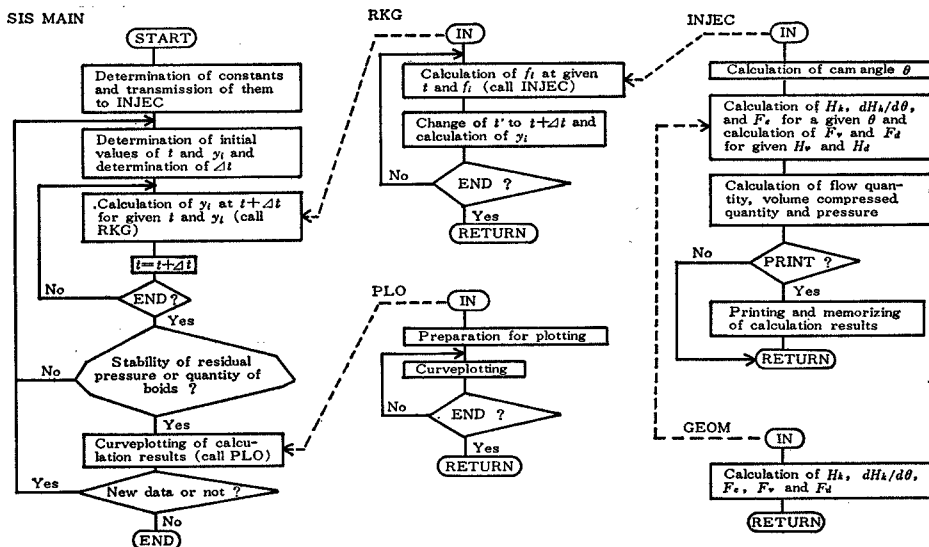


Fig. 2. Program of fuel injection system shown in flow chart

system can not be estimated at the first calculation cycle as the initial conditions, the calculation is set about assuming an arbitrary residual pressure, practically zero. The calculating cycles are repeated until the residual pressure before an injection takes the same value as that after the injection. Unless the injection characteristic shows the irregular or nearly irregular injection, the residual pressure or the quantity of boids becomes constant when the calculations are repeated four or five cycles.

The program to obtain numerical solutions of the Eqs. (1) to (18) consists of one main- and five sub-programs. The flowchart of this program is shown in Fig. 2.

#### 4. Calculated Results and Their Comparisons with Experimental Results

The main specifications of the fuel injection system used in this investigation are:

Pump section: Bosch overflow type (plunger dia.=16 mm and see Figs. 3, 4 and 5)

Nozzle section: hole type nozzle (0.4×8 holes and see Fig. 6)

Pipe line section: 3 mm I.D. and 980 mm length.

The operating conditions are the cam speed  $n=750$  rpm, the nozzle opening pressure  $p_o=300$  kg/cm<sup>2</sup>, the pump feed pressure  $p_e=2.0$  kg/cm<sup>2</sup>, the effective plunger stroke  $rack=0.3$  cm and the back pressure at nozzle  $p_z=90$  kg/cm<sup>2</sup>. The fuel used in this study is A-heavy oil ( $\rho=0.855$  kg·s/cm<sup>4</sup> and  $\nu=7.4$  cts. at 20°C).

Prior to calculating the characteristics of an injection system according to the procedure described in Sec. 3, it is necessary to give the characteristic values. These standard values are shown in Table 1. In this section, we show how the characteristic values affect the performances of fuel injection system. The calculated injection characteristics, especially pressure in a pipe line, nozzle needle valve lift and rate of

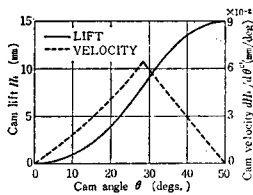


Fig. 3. Cam lift and velocity curves

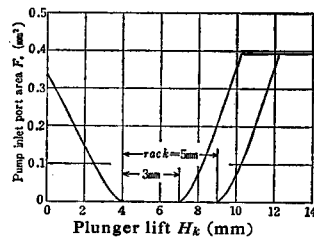


Fig. 4. Pump inlet area vs. plunger lift

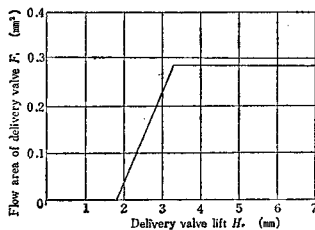


Fig. 5. Flow area vs. lift of delivery valve

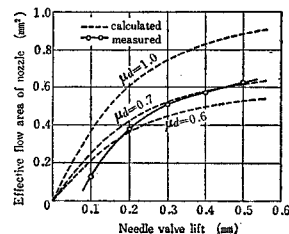


Fig. 6. Effective flow area of nozzle

Table 1. Characteristic Values Used in Calculation

Inlet port discharge coefficient	$\mu_e$	0.6	—
Delivery valve discharge coefficient	$\mu_v$	0.6	—
Delivery valve damping factor	$K_v$	0.04	kg-s/cm
Nozzle discharge coefficient	$\mu_d$	0.6	—
Nozzle damping factor	$K_d$	0.05	kg-s/cm
Resistance coefficient in a pipe line	$\zeta$	200	—
Sound velocity in fuel	$a$	$1.45 \times 10^3$	cm/s

injection are compared with the standard ones.

(1) Number of calculating loops (LOOP): Since the residual pressure or the quantity of boids in a system is unknown, the residual pressure is assumed to be zero at the beginning of calculations. After accomplishing the calculation of the first loop, the residual pressure obtained is applied to the second loop as an initial value and several loops are iterated in a similar manner. If the difference between the assumed and the obtained residual pressures in a calculation loop becomes less than a value set in advance, the iteration stops and the calculated results of the last injection loop are regarded as the ones under this operating condition. On practical calculations, the residual pressure converges to a certain constant value after three or four iterations of the loops, if the operating condition is normal. Fig. 7 illustrates the progress of the convergence in residual pressures and injection quantities under the normal and the irregular injection.

(2) Time interval (STEP) and number of division of equivalent pipe line (N): As

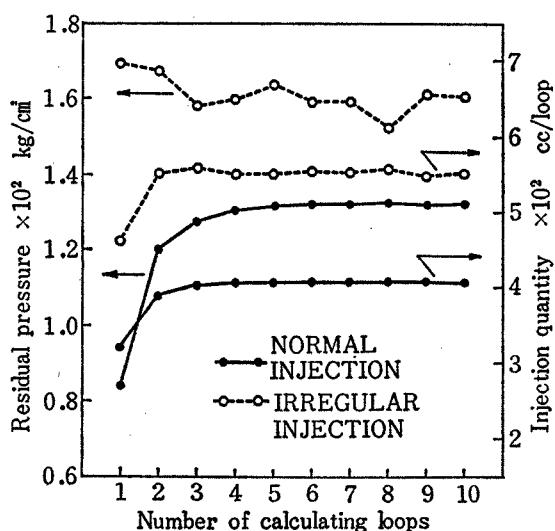


Fig. 7. Convergence of residual pressure and injection quantity



shown in Sec. 2.6, the equivalent pipe line ( $L$ ) (see Fig. 1) is divided into a finite number of elements, each of which is regarded as a lumped parameter system in calculation. The differential equations can be integrated numerically and solved by a finite difference method. Thus, the number of division and the time interval will affect the calculated results. For larger  $N$  and smaller  $STEP$ , it will take wastefully a long time to calculate. On the contrary, for smaller  $N$  and larger  $STEP$ , the rough results will be obtained. The values of  $N$  and  $STEP$  assumed as a standard are 8 and 0.05 ms, respectively. Under these conditions, the pressure waves pass through one element for about two steps, where the sound velocity in the fuel is assumed to be 1450 m/s. Under states of the valve which is above the restricted lift and at the seat,  $STEP$  is furthermore subdivided.

Fig. 8 shows the effects of  $N$  and  $STEP$  on major injection characteristics, that is, the pressure in the line (at the point of 987 mm from the exit of the delivery chamber), the nozzle needle valve lift and the injection rate. As increasing  $N$  from 4 to 12, the higher components of frequency appear both in the injection rate and in the pressure in the line, but the effect of  $N$  is small as a whole. It should be, however, noted that a larger  $N$  must be applied for a longer pipe line. When calculating with the half of the standard time interval (0.025 ms), the pressure in the line vibrates with a high frequency and since the pipe line pressure near the end of the primary injection is smaller than the standard, the negative injection rate, namely, the back-

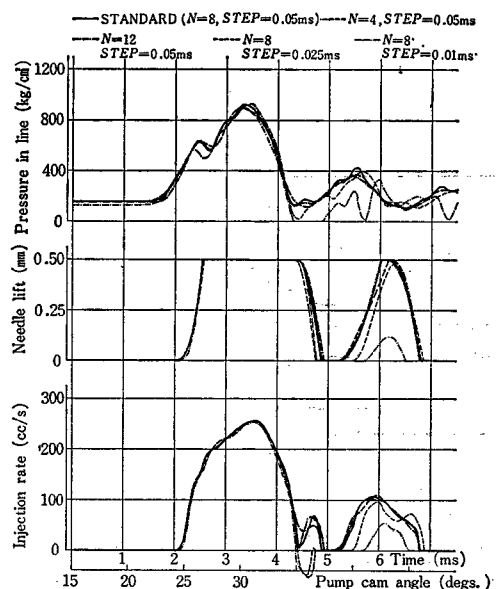


Fig. 8. Effects of calculation step and number of division of pipe line on injection characteristics ( $n=750$  rpm,  $rack=0.3$  cm)

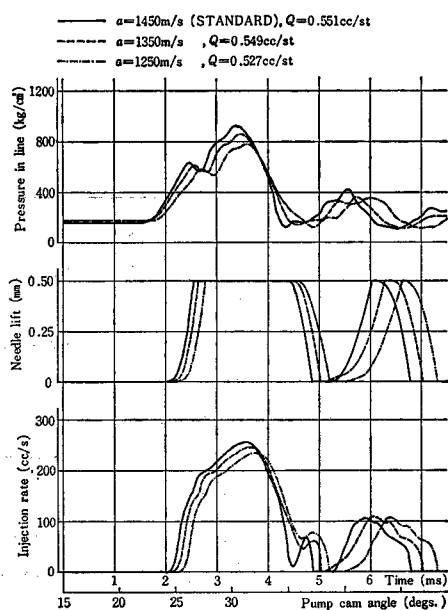


Fig. 9. Effects of sound velocity ( $n=750$  rpm,  $rack=0.3$  cm)

flowing at needle valve is observed there. For the smaller *STEP* (0.01 ms), the fuel line pressure becomes zero near the end of the primary injection. This phenomenon shows the generation of boids in the system. The secondary injection decreases considerably. From the facts mentioned above, the optimum *N* and *STEP* should be decided according to the operating conditions and the dimensions of the system.

(3) Sound velocity in fuel (*a*): Fig. 9 shows the calculated results under the conditions of *a*=1450 (standard), 1350, 1250 m/s. As *a* decreases, the rising of the curves of the pressure, the valve lift and the injection rate is delayed and the maximum values of the pressure and the injection rate decrease. The quantity of secondary injection is little affected by a change of the sound velocity.

(4) Resistance coefficient in fuel pipe line ( $\zeta$ ): The standard value of  $\zeta$  estimated by Eq. (11) is 200 in the system used in this study. It is obvious for large  $\zeta$  in Fig. 10 that the maximum pressure in the line decreases due to a increase of the friction between the fuel and the pipe wall, and that a small pressure drop after the maximum pressure and a smooth pressure history after the primary injection are obtained. Especially for  $\zeta=600$ , the injection rate is high at the end of the primary injection, and the primary and the secondary injections are observed continuously, but the overall durations of injection are the same.

(5) Discharge coefficients ( $\mu_e$ ; at pump inlet ports,  $\mu_v$ ; at delivery valve,  $\mu_d$ ; at nozzle needle valve): As shown in Eqs. (4), (5) and (15), the effective flow area at the orifice can be represented by a product of the discharge coefficient and the geometrical flow area. All of the discharge coefficients are assumed 0.6 as a standard

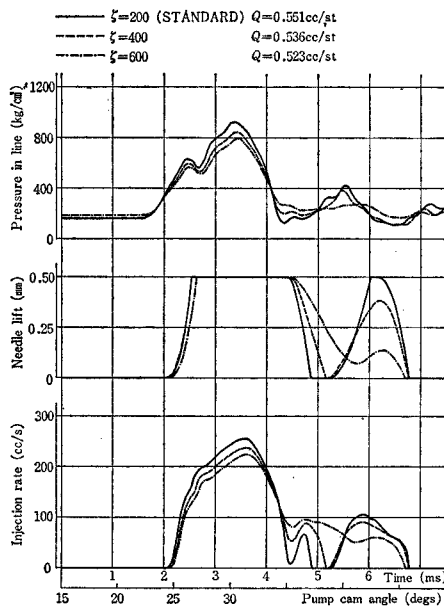


Fig. 10. Effects of friction factor ( $n=750$  rpm, rack=0.3 cm)

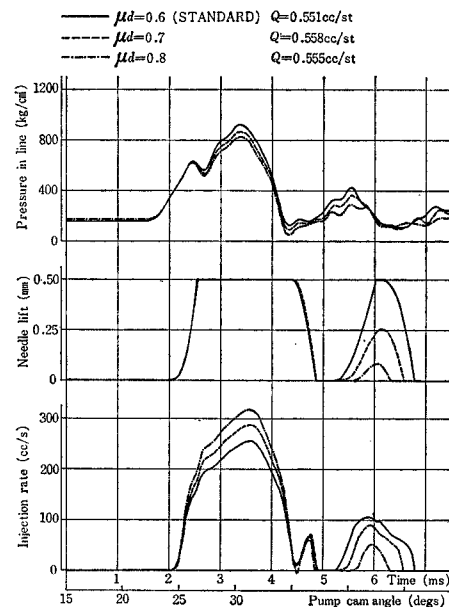


Fig. 11. Effects of nozzle discharge coefficient ( $n=750$  rpm, rack=0.3 cm)

value and a comparison of calculated results for 0.6, 0.7 and 0.8 is made. For inlet ports of the plunger chamber, the effect of  $\mu_e$  on injection characteristics is relatively small because there is enough time to charge a plunger chamber with the fuel and because the pressure in the plunger chamber before the port closes is little affected by the change of  $\mu_e$ . The effect of  $\mu_v$  is also small. Fig. 11 shows the calculated results for different  $\mu_d$ , where the geometrical area includes the area between the needle valve and the seat and the area of the nozzle holes. As  $\mu_d$  or the effective area at the nozzle increases, the peak of the primary injection becomes high. Since the primary injection quantity increases with an increase in  $\mu_d$ , the secondary injection quantity tends to be small.

(6) Damping factors of valves ( $K_v$ ; at delivery valve,  $K_d$ ; at nozzle needle valve): It is troublesome to estimate the damping factors of the valves among the characteristic values shown in Table 1 because of few data related to these values and of dissimilarity of its type or its dimension. The values of the damping factor in Table 1 are those proposed by Huber and Schaffiz<sup>4)</sup> which are similar to the valve of this study in the shape of the retraction type delivery valve and the multi-hole type nozzle. Fig. 12 illustrates the calculated results for  $K_v=0.04, 0.10$ , and  $0.15$  kg·s/cm under constant  $K_d$  of  $0.05$  kg·s/cm. With an increase of  $K_v$ , the gradient of the delivery valve lift curve is smaller and the closing points of the valve are retarded. These phenomena can be explained as follows; the last term of the right hand side in Eq. (8) is the damping force which acts on the delivery valve in a reverse

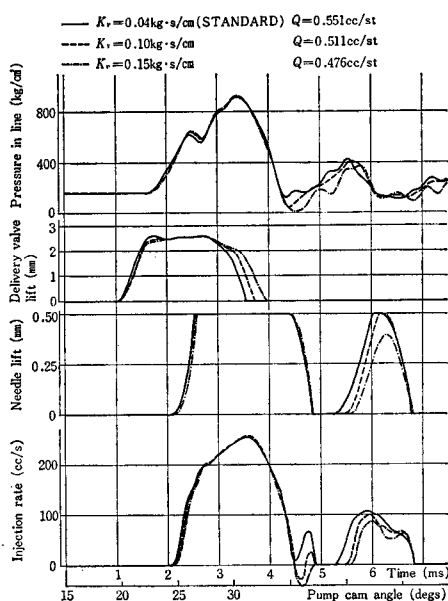


Fig. 12. Effects of damping factor at delivery valve ( $n=750$  rpm, rack=0.3 cm)

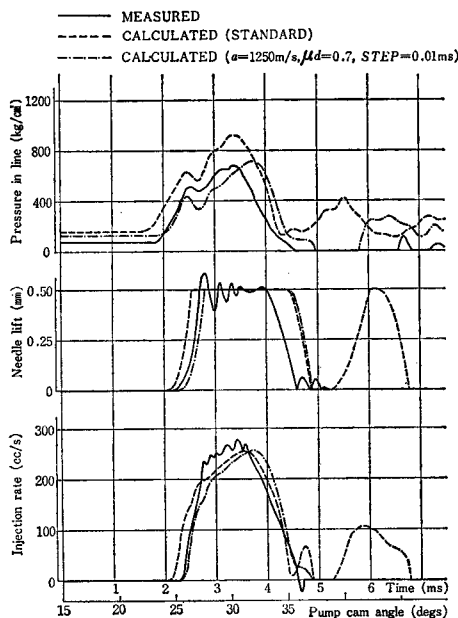


Fig. 13. Comparison between calculated and experimental results ( $n=750$  rpm, rack=0.3 cm)

direction to the motion of the valve. With an increase of  $K_v$ , since the damping force increases, the duration required from the maximum lift to the retraction stroke (1.8 mm) becomes long, so that the quantity of the fuel flow from the delivery chamber into the plunger chamber becomes large. Thus, the pressure drop in the pipe line near the end of the primary injection causes a negative injection rate and in an actual engine it corresponds to the suction of air from the combustion chamber. However, by back-flowing at the delivery valve near the primary injection end, in other words by a pressure drop in the line, the reflection pressure waves are lowered and the secondary injection becomes small. Since the effect of  $K_d$  on injection characteristics is small, the comparisons are omitted.

#### (7) Comparison with experimental results

In order to verify the calculated results, simple experiments were performed. Measurements were carried out chiefly on the injection quantity per one pump stroke, the pressure in the fuel pipe line, the nozzle needle valve lift and the injection rate. The injection quantity was measured by the flowmeter, the pressure in the line was measured by the strain gauge type pressure transducer mounted on the pipe line at 987 mm from the outlet of the delivery valve and the needle valve lift was detected by the induction type non-contact vibration pickup. Measurement of the injection rate was made by Bosch's method which is said to be of simple construction and of high accuracy, keeping the back pressure of the nozzle at 90 kg/cm<sup>2</sup>.

The experimental results are shown by solid lines in Fig. 13 compared with the calculated results shown by broken lines under  $n=750$  rpm and  $rack=0.3$  cm. The calculated pressure in the pipe line is very high and the generation of boids is not observed and larger amounts of the secondary injection take place as compared with the experimental results. As we can see from this comparison, there is a large discrepancy. The calculated results obtained by the measured sound velocity and the measured nozzle discharge coefficient are also shown by dot-dash-lines in Fig. 13. It is clearly seen that the mutual relation between the experiment and the calculation is fairly improved.

### 5. Conclusions

At the simulation of the fuel injection system in diesel engines, the authors showed the assumptions, the basic equations, the procedures of calculation, the effects of several characteristic values on injection performances and a comparison of calculation with experiment. The conclusions are summarized as follows:

- (1) The optimum values should be given for the basic factors such as the number of calculating loops, the number of division of the pipe line and the time interval according to the dimensions and the operating conditions of the system.
- (2) The influences of changes of various characteristic values on injection performances were ascertained as follows:

(a) The pressure in the fuel pipe line decreases with a decrease in the sound velocity in the fuel and with an increase in the resistance coefficient of the pipe line and in the discharge coefficient at the nozzle.

(b) The secondary injection decreases with an increase in the discharge coefficient at the nozzle and in the damping factor at the delivery valve.

(c) The other characteristic values little affected the injection performances.

(3) The qualitative correlation between the calculated and the experimental results was good. Furthermore, the sound velocity and the discharge coefficient at the nozzle were measured and the calculated results with those observed values agreed fairly well with the experimental results.

This simulator of the fuel injection system will be improved furthermore, if these characteristic values are estimated more precisely. We believe this model outlined in this paper can be applied effectively to the other types of injection system under considerations of the effects of the fundamental factors and the characteristic values on the injection performances.

#### Notation

$a$	sound velocity	(cm/s)
$c$	stiffness of valve spring	(kg/cm)
$E$	elastic modulus of fuel	(kg/cm <sup>2</sup> )
$F$	area	(cm <sup>2</sup> )
$H$	lift of valve or stroke	(cm)
$K$	damping factor of valve	(kg·s/cm)
$L$	length of pipe line	(cm)
$m$	mass	(kg·s <sup>2</sup> /cm <sup>4</sup> )
$N$	a number of divided elements of fuel pipe line	
$n$	revolution per minute of cam shaft	(rpm)
$p$	pressure	(kg/cm <sup>2</sup> )
$Q$	quantity of injection	(cm <sup>3</sup> )
$q$	rate of flow or rate of injection	(cm <sup>3</sup> /s)
$rack$	effective plunger stroke	(cm)
$s$	quantity of fuel compressed in an element	(cm <sup>3</sup> )
$t$	time	(s)
$V$	volume	(cm <sup>3</sup> )
$\zeta$	resistance coefficient	
$\nu$	viscosity coefficient at orifice	
$\theta$	cam angle	(rad)
$\mu$	discharge coefficient at orifice	
$\rho$	density of fuel	(kg·s/cm <sup>4</sup> )

#### Subscripts

$e$	feeding duct
-----	--------------

$d$	nozzle holder or nozzle
$k$	plunger or pumping chamber
$l$	pipe line
$v$	delivery valve or delivery chamber
$o$	situation of zero stroke or initial condition

[illegible]

**Fig. A. Symbols and subscripts**

The authors would like to express their appreciation to Professor Ikegami at Kyoto University for providing the samples and his helpful advices. This study was supported financially in part by Study Group of SR 122 in the Marine Engineering Society in Japan. The calculation were carried out at the Computer Center of University of Osaka Prefecture.

- 1) B.E. Knight: PIME (AD), No. 1 (1960-61).
- 2) W. Vogel; MTZ, Jg. 24, Nr. 1 (1963).
- 3) G. Sitkei; Kraftstoffaufbereitung und Verbrennung bei Dieselmotoren, Springer (1964).
- 4) F.W. Huber und W. Schaffiz; MTZ, Jg. 27, Nr. 4 (1968).
- 5) H. Hiroyasu et al; Bull of JSME, Vol. 34, No. 260 (1968).
- 6) F. Nagao et al; Preprint of JSME, No. 44-9 (1969).
- 7) G.A. Becchi; SAE Paper, 710568 (1971).
- 8) Y. Hirako et al; Bull of MESJ, Vol. 2, No. 2 (1974).
- 9) U. Fujihira et al; Preprint of JSME, No. 694 (1961).
- 10) M. Tateishi et al; Preprint of JSME, No. 714-5 (1971).
- 11) T. Kushiyaama et al; Preprint of JSME, No. 714-5 (1971).